J|A|C|S
ARTICLES
Published on Web 12/20/2006

# Elucidation of Hydrolysis Mechanisms for Fatty Acid Amide Hydrolase and Its Lys142Ala Variant via QM/MM Simulations

Ivan Tubert-Brohman, Orlando Acevedo, and William L. Jorgensen*

*Contribution from the Department of Chemistry, Yale University, New Haven, Connecticut 06520-8107*

Received August 11, 2006; E-mail: william.jorgensen@yale.edu

***Abstract:*** Fatty acid amide hydrolase (FAAH) is a serine hydrolase that degrades anandamide, an endocannabinoid, and oleamide, a sleep-inducing lipid, and has potential applications as a therapeutic target for neurological disorders. Remarkably, FAAH hydrolyzes amides and esters with similar rates; however, the normal preference for esters reemerges when Lys142 is mutated to alanine. To elucidate the hydrolysis mechanisms and the causes behind this variation of selectivity, mixed quantum and molecular mechanics (QM/MM) calculations were carried out to obtain free-energy profiles for alternative mechanisms for the enzymatic hydrolyses. The methodology features free-energy perturbation calculations in Monte Carlo simulations with PDDG/PM3 as the QM method. For wild-type FAAH, the results support a mechanism, which features proton transfer from Ser217 to Lys142, simultaneous proton transfer from Ser241 to Ser217, and attack of Ser241 on the substrate's carbonyl carbon to yield a tetrahedral intermediate, which subsequently undergoes elimination with simultaneous protonation of the leaving group by a Lys142-Ser217 proton shuttle. For the Lys142Ala mutant, a striking multistep sequence is proposed with simultaneous proton transfer from Ser241 to Ser217, attack of Ser241 on the carbonyl carbon of the substrate, and elimination of the leaving group and its protonation by Ser217. Support comes from the free-energy results, which well reproduce the observation that the Lys142Ala mutation in FAAH decreases the rate of hydrolysis for oleamide significantly more than for methyl oleate.

## Introduction

Fatty acid amide hydrolase (FAAH)[1−3] is an integral membrane protein responsible for the degradation of fatty acid primary amides and ethanolamides such as anandamide and oleamide (Figure 1).[4,5] Anandamide binds and activates the cannabinoid receptors CB1 and CB2 as well as the vanilloid receptor VR1 through which it is thought to exert its analgesic and cannabinoid effects,[6−9] and oleamide has been found to accumulate under conditions of sleep deprivation and to induce sleep in animals.[10,11] FAAH constitutes the only characterized mammalian member of the amidase signature family, a class of serine hydrolases that bear a unique catalytic triad, Ser-Ser-Lys,[12,13] and is notable for its ability to hydrolyze amides and esters with similar rates. This selectivity is believed to have

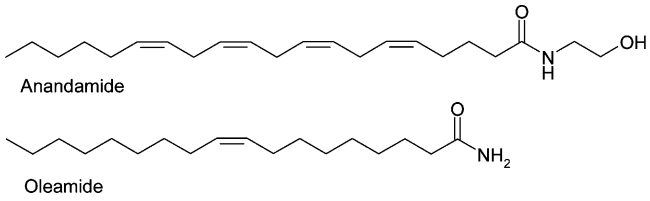


***Figure 1.*** Structures of anandamide and oleamide.

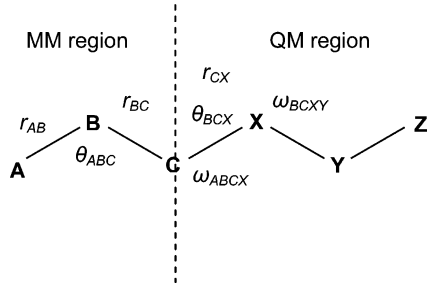


***Figure 2.*** MM bonded energy terms near the QM/MM interface. The QM link atom is placed coincident with the MM atom **C**.

(1) Cravatt, B. F.; Giang, D. K.; Mayfield, S. P.; Boger, D. L.; Lerner, R. A.; Gilula, N. B. *Nature* **1996**, *384*, 83−87.
(2) Giang, D. K.; Cravatt, B. F. *Proc. Natl. Acad. Sci. U.S.A.* **1997**, *94*, 2238−2242.
(3) Patricelli, M. P.; Cravatt, B. F. *Vitam. Horm. (San Diego, CA, U.S.)* **2001**, *62*, 95−131.
(4) Boger, D. L.; Fecik, R. A.; Patterson, J. E.; Miyauchi, H.; Patricelli, M. P.; Cravatt, B. F. *Bioorg. Med. Chem. Lett.* **2000**, *10*, 2613−2616.
(5) Lang, W.; Qin, C.; Lin, S.; Khanolkar, A. D.; Goutopoulos, A.; Fan, P.; Abouzid, K.; Meng, Z.; Biegel, D.; Makriyannis, A. *J. Med. Chem.* **1999**, *42*, 896−902.
(6) Martin, B. R.; Mechoulam, R.; Razdan, R. K. *Life Sci.* **1999**, *65*, 573−595.
(7) Axelrod, J.; Felder, C. C. *Neurochem. Res.* **1998**, *23*, 575−581.
(8) Zygmunt, P. M.; Petersson, J.; Andersson, D. A.; Chuang, H.-H.; Sorgard, M.; Di Marzo, V.; Julius, D.; Hogestatt, E. D. *Nature* **1999**, *400*, 452−457.
(9) Smart, D.; Gunthorpe, M. J.; Jerman, J. C.; Nasir, S.; Gray, J.; Muir, A. I.; Chambers, J. K.; Randall, A. D.; Davis, J. B. *Br. J. Pharmacol.* **2000**, *129*, 227−230.
(10) Cravatt, B. F.; Prospero-Garcia, O.; Siuzdak, G.; Gilula, N. B.; Henriksen, S. J.; Boger, D. L.; Lerner, R. A. *Science* **1995**, *268*, 1506−1509.
(11) Huitron-Resendiz, S.; Gombart, L.; Cravatt, B. F.; Henriksen, S. J. *Exp. Neurol.* **2001**, *172*, 235−243.
(12) Bracey, M. H.; Hanson, M. A.; Masuda, K. R.; Stevens, R. C.; Cravatt, B. F. *Science* **2002**, *298*, 1793−1796.
(13) McKinney, M. K.; Cravatt, B. F. *J. Biol. Chem.* **2003**, *278*, 37393−37399.


**10.1021/ja065863s CCC: $33.50** 

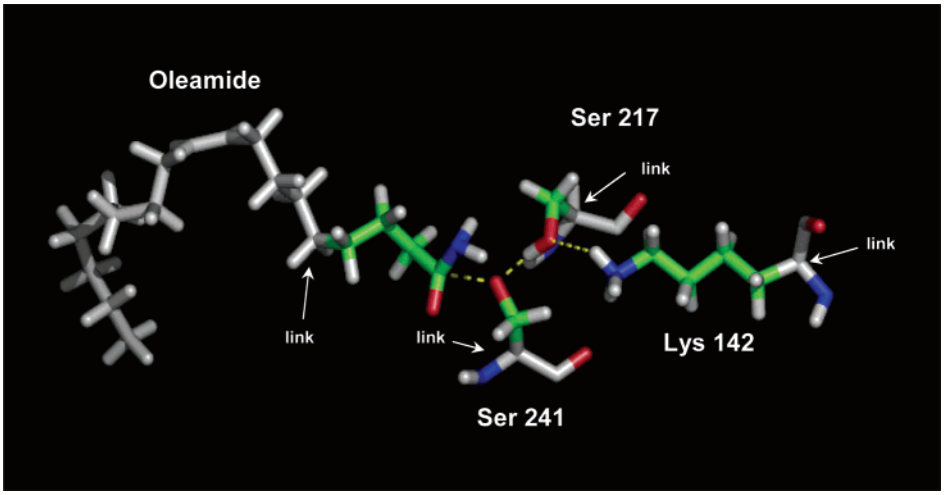


***Figure 3.*** Active site of FAAH with oleamide as substrate. The QM region consists of the carbon atoms shown in green, their attached hydrogen atoms, and the terminal functional groups. The hydrocarbon tail of oleamide resides in a hydrophobic channel; see ref 12 for details.

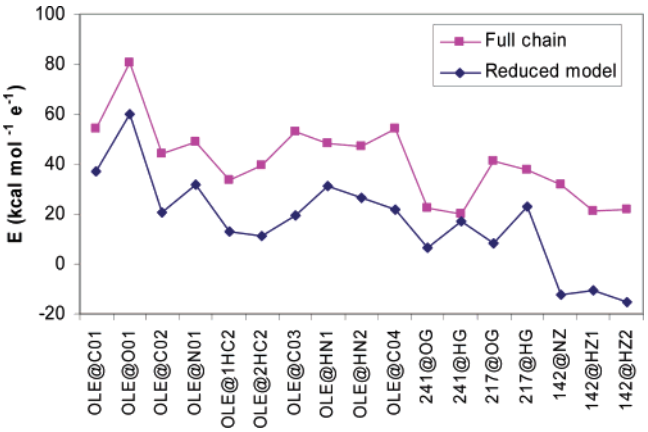


***Figure 4.*** Comparison of the electric potential on selected atoms between the reduced and the full chain model. OLE refers to the oleamide substrate.

evolved to allow the enzyme to control the magnitude and duration of signals communicated by endogenous fatty acid amides within a complex milieu of structurally similar lipid natural products.[13] Because of its metabolic role and unique mechanism, FAAH is a potential therapeutic target for treating pain, sleep disorders, and related neurological irregularities.[14,15] Considerable effort has been invested into elucidating the detailed mechanism of hydrolysis by FAAH, as a better understanding could aid in the design of new inhibitors. Most of the available experimental data about the mechanism comes from kinetic studies of wild-type FAAH and mutants where the active site residues Lys142, Ser217, and Ser241 have been modified.[13] A key observation from the site-directed mutagenesis study was that replacing Lys142 with alanine has very different effects on the hydrolysis rates of oleamide and methyl oleate; the Lys142Ala mutant hydrolyzes oleamide and methyl oleate 104 000 and 600 times slower, respectively, than wild-type FAAH.[13]

The three-dimensional structure of FAAH has been recently determined by X-ray crystallography.[12] This allowed our group to examine striking variations in the inhibition of FAAH by α-ketoheterocycle derivatives using Monte Carlo (MC) simulations and free-energy perturbation (FEP) theory to compute relative free energies of binding.[16,17] The structure was also used by Lodola et al. to construct a potential energy map for the first steps of the hydrolysis of oleamide by FAAH using quantum mechanics/molecular mechanics (QM/MM) energy minimizations;[18] specifically, they modeled the proton transfer and addition steps proposed by McKinney and Cravatt leading to the tetrahedral intermediate.[13]

The aim of this work is to explore the hydrolysis mechanism more thoroughly, with particular emphasis on elucidating the causes behind the different sensitivities of the hydrolysis rates of oleamide and methyl oleate toward mutation of Lys142. Thus, the hydrolysis of both oleamide and methyl oleate by both wild-type and Lys142Ala FAAH have been modeled. Furthermore, the present QM/MM/MC/FEP calculations include extensive sampling of the substrate, protein, and hundreds of water molecules to obtain configurationally averaged free-energy changes as opposed to energy minimizations, which do not include entropy effects and are sensitive to starting geometries. In addition, several mechanisms for the hydrolyses by FAAH were considered in order to clarify the sequence of proton-transfer steps and whether the addition or elimination part of the acylation is rate-limiting. The acylation step is considered to be rate-determining for the overall hydrolysis according to kinetic data.[13]

## Computational Methods

**QM/MM Method.** A QM/MM method describes the reactive part of the system quantum mechanically, while the environment is treated classically using molecular mechanics.[19−21] In the present implementation, the nonbonded interactions between the QM part of the system

(14) Cravatt, B. F.; Lichtman, A. H. *Curr. Opin. Chem. Biol.* **2003**, *7*, 469−475.
(15) Maccarrone, M. *Curr. Pharm. Des.* **2006**, *12*, 759−772.
(16) Guimarães, C. R. W.; Boger, D. L.; Jorgensen, W. L. *J. Am. Chem. Soc.* **2005**, *127*, 17377−17384.
(17) Boger, D. L.; Miyauchi, H.; Du, W.; Hardouin, C.; Fecik, R. A.; Cheng, H.; Hwang, I.; Hedrick, M. P.; Leung, D.; Acevedo, O.; Guimaraes, C. R. W.; Jorgensen, W. L.; Cravatt, B. F. *J. Med. Chem.* **2005**, *48*, 1849−1856.
(18) Lodola, A.; Mor, M.; Hermann, J. C.; Tarzia, G.; Piomelli, D.; Mulholland, A. J. *Chem. Commun.* **2005**, 4399−4401.
(19) Aqvist, J.; Warshel, A. *Chem. Rev.* **1993**, *93*, 2523−2544.
(20) Gao, J.; Ma, S.; Major, D. T.; Nam, K.; Pu, J.; Truhlar, D. G. *Chem. Rev.* **2006**, *106*, 3188−3209.
(21) Kaminski, G. A.; Jorgensen, W. L. *J. Phys. Chem. B* **1998**, *102*, 1787−1796.

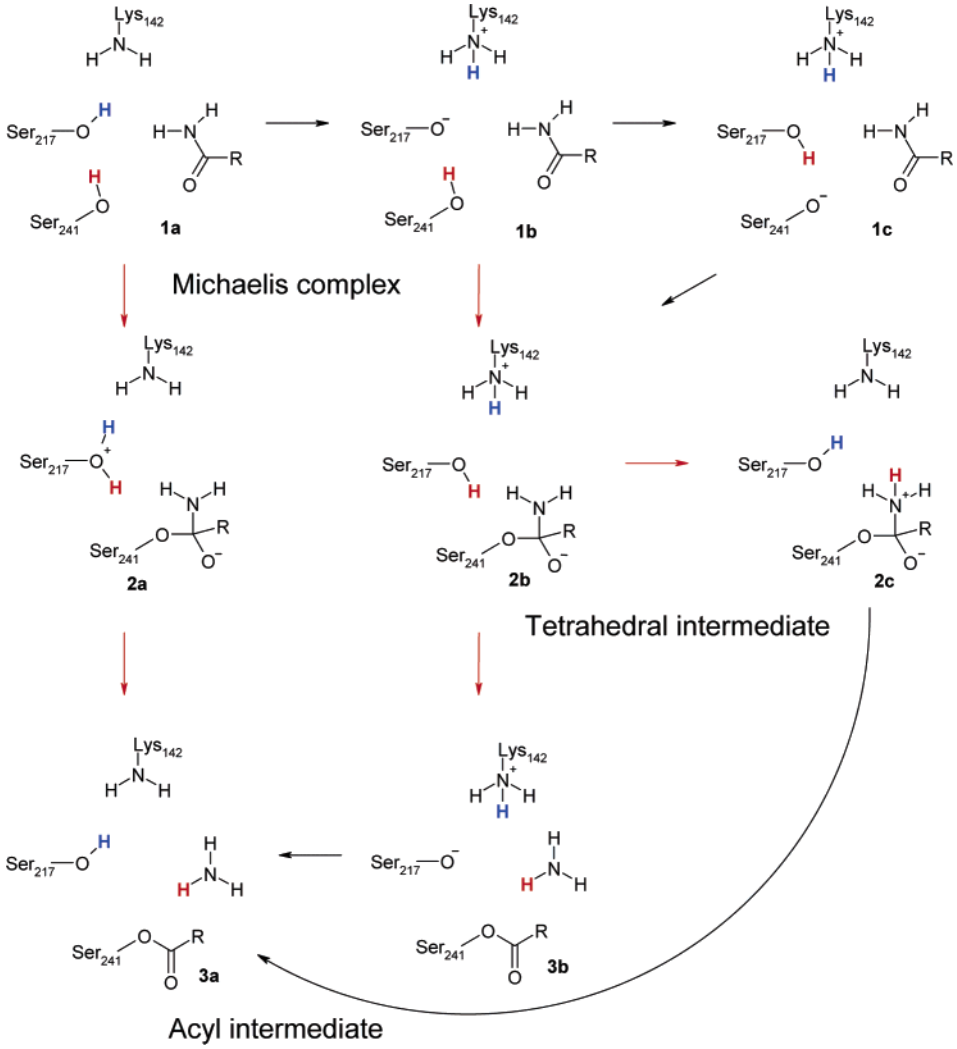


***Figure 5.*** Reaction pathways considered in this work. The processes with red and black arrows were studied using 2D and 1D PMF calculations, respectively. The protons undergoing transfer are highlighted in red and blue.

and its environment are treated classically, using eq 1

$$E_{QM/MM} = \sum_{i}^{\text{onQM}} \sum_{j}^{\text{onMM}} [q_i q_j e^2/r_{ij} + 4\epsilon_{ij}(\sigma^{12}/r_{ij}^{12} - \sigma^6/r_{ij}^6)] \quad (1)$$

where $q_i$ and $q_j$ are the partial atomic charges, and $\sigma_{ij}$ and $\epsilon_{ij}$ are Lennard−Jones parameters. This approach has already been used successfully for the simulation of reactions in solution and in protein systems.[22−28] A major issue for QM/MM calculations that involve covalent bonds between the QM part of the system and the MM part is the "capping" of the QM region and the treatment of bonded interactions near the interface. Two popular approaches are the link atom[29−31] and the local self-consistent field formalisms.[32−34] The approach used in this work is very similar to the one used by Guimarães et al. for simulations of macrophomate synthase;[35] it consists of a modified link-atom approach and is implemented in the MCPRO package.[36] For the covalent QM/MM interface, the QM system is capped with a hydrogen atom, placed coincident with the adjacent MM atom (atom **C** in Figure 2). The partial charge from the link atom is added to QM-atom **X**; this results in a charge distribution similar to that from the OPLS-AA force field. Figure 2 also shows the MM terms that can be included in the potential energy function. The artificial elongation of the X−H bond does not affect the charges significantly but does result in a large increase of the QM energy. This increase, however, is kept constant by not sampling the bonds and angles involving atom **X**. Consequently, MM energy terms such as $r_{CX}$ and $\theta_{BCX}$ do not need to be added to the potential energy function because they would also represent a constant contribution. Nonbonded intramolecular energy terms between the QM region and the MM region are only included when the two atoms are at least three bonds away, and 1,4 interactions are scaled by a factor of 0.5, as is conventional for the OPLS-AA force field.[37]

(22) Acevedo, O.; Jorgensen, W. L. *Org. Lett.* **2004**, *6*, 2881−2884.
(23) Acevedo, O.; Jorgensen, W. L. *J. Am. Chem. Soc.* **2005**, *127*, 8829−8834.
(24) Acevedo, O.; Jorgensen, W. L. *J. Am. Chem. Soc.* **2006**, *128*, 6141−6146.
(25) Acevedo, O.; Jorgensen William, L. *J. Org. Chem.* **2006**, *71*, 4896−4902.
(26) Guimarães, C. R. W.; Repasky, M., P.; Chandrasekhar, J.; Tirado-Rives, J.; Jorgensen, W. L. *J. Am. Chem. Soc.* **2003**, *125*, 6892−6899.
(27) Guimarães, C. R. W.; Udier-Blagovic, M.; Tubert-Brohman, I.; Jorgensen, W. L. *J. Chem. Theory Comput.* **2005**, *1*, 617−625.
(28) Repasky, M. P.; Guimaraes, C. R. W.; Chandrasekhar, J.; Tirado-Rives, J.; Jorgensen, W. L. *J. Am. Chem. Soc.* **2003**, *125*, 6663−6672.
(29) Singh, U. C.; Kollman, P. A. *J. Comput. Chem.* **1986**, *7*, 718−730.
(30) Field, M. J.; Bash, P. A.; Karplus, M. *J. Comput. Chem.* **1990**, *11*, 700−733.
(31) Eurenius, K. P.; Chatfield, D. C.; Brooks, B. R.; Hodoscek, M. *Int. J. Quantum Chem.* **1996**, *60*, 1189−1200.
(32) Thery, V.; Rinaldi, D.; Rivail, J. L.; Maigret, B.; Ferenczy, G. G. *J. Comput. Chem.* **1994**, *15*, 269−282.
(33) Monard, G.; Loos, M.; Thery, V.; Baka, K.; Rivail, J. L. *Int. J. Quantum Chem.* **1996**, *58*, 153−159.
(34) Reuter, N.; Dejaegere, A.; Maigret, B.; Karplus, M. *J. Phys. Chem. A* **2000**, *104*, 1720−1735.
(35) Guimarães, C. R. W.; Udier-Blagovic, M.; Jorgensen, W. L. *J. Am. Chem. Soc.* **2005**, *127*, 3577−3588.
(36) Jorgensen, W. L.; Tirado-Rives, J. *J. Comput. Chem.* **2005**, *26*, 1689−1700.

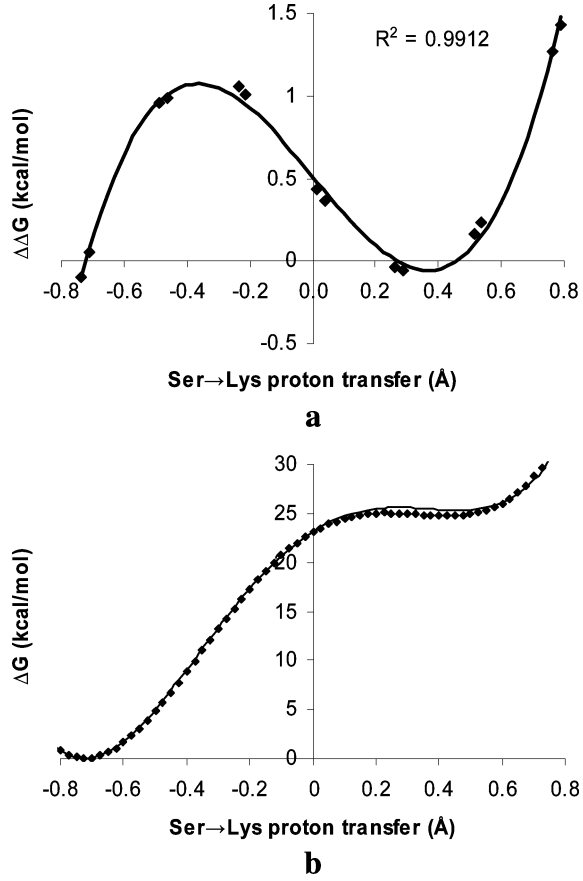


***Figure 6.*** For proton transfers, the changes in $\Delta G$ for seven individual windows (a) are fitted by a cubic polynomial, which is integrated analytically to give the full PMF (b, solid line). The "exact" PMF using 33 windows is shown for comparison (b, dotted line).

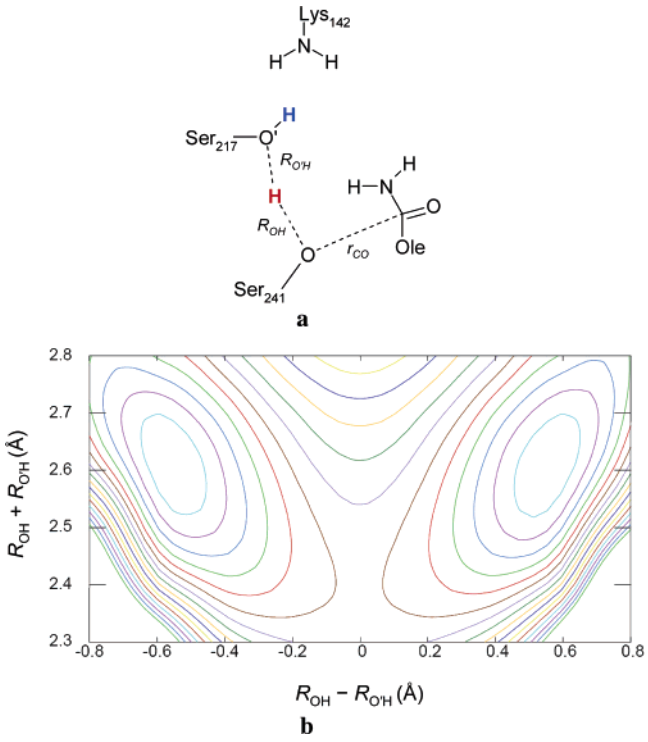


***Figure 7.*** (a) Reaction coordinates for the transformation of structure **1a** to **2a**. One variable is $R_{CO}$, representing the addition of the Ser214 oxygen to the oleamide carbonyl; the other is the combination $R_{OH} - R_{O'H}$ with $R_{OH} + R_{O'H}$ kept constant at 2.6 Å, which represents the Ser241 → Ser217 proton transfer. (b) Gas-phase potential energy surface for the proton transfer between protonated methanol and methanol, computed using PDDG/PM3. Contour lines are spaced every 1 kcal/mol.

***Table 1.*** Computed Free Energies of Reaction and Activation (kcal/mol) for Each Step of Oleamide Hydrolysis by FAAH

| step | $\Delta G^{\ddagger}$ | $\Delta G$ |
|---|---|---|
| **1a** → **1b** | 25.1 ± 0.1 | 24.8 ± 0.1 |
| **1a** → **2a** | 36.9 ± 0.5 | 27.2 ± 0.5 |
| **1b** → **1c** | 17.6 ± 0.5 | 10.4 ± 0.5 |
| **1b** → **2b** | 7.6 ± 0.1 | −25.2 ± 0.5 |
| **1c** → **2b** | 0 | −37.0 ± 0.5 |
| **2a** → **3a** | 0 | −42.8 ± 0.5 |
| **2b** → **2c** | 24.3 ± 0.5 | −3.1 ± 0.5 |
| **2b** → **3b** | 17.7 ± 0.5 | 12.4 ± 0.5 |
| **2c** → **3a** | 0.7 ± 0.5 | −14.6 ± 0.5 |
| **3b** → **3a** | 0.3 ± 0.5 | −28.0 ± 0.5 |

For the QM part of the system, a very fast QM method is essential due to the extensive Monte Carlo sampling. The PDDG/PM3 semiempirical method[38−40] was chosen in light of its improved accuracy over the popular AM1[41] and PM3[42] methods and because of its successful application for other QM/MM simulations of reactions in solution.[22−25] For the QM atomic charges, the CM3 charge model[43] is used with the charges scaled by a factor of 1.12, which has been optimized to reproduce experimental free energies of hydration.[44] The QM region here does not have a net charge.

**QM/MM System.** The QM region used for the simulation of oleamide hydrolysis by FAAH includes the side chains of Lys142, Ser217, and Ser241, as well as the substrate up to C4 (Figure 3). The total composition is represented by the formula $C_{10}H_{28}N_2O_3$. There are four link atoms: the three α-carbons of the active site residues and C5 of oleamide. A similar QM region was used for the simulations involving methyl oleate; for simulations involving the Lys142Ala mutant, Ala142 was entirely in the MM region. The latest QM/MM implementation in MCPRO supports movable (i.e., they can be varied during the MC simulations) link atoms, which made it possible to exclude most of the oleamide/oleate hydrocarbon chain. Given the cubic scaling for execution time common for semiempirical methods, it is estimated that this results in an 8-fold increase in the speed of the QM calculations.

The initial Cartesian coordinates for the protein−ligand complex were derived from those used in our previous study of FAAH inhibition.[16] The 2.8-Å crystal structure of FAAH complexed to methoxyarachidonyl phosphonate (MAP), with PDB id 1mt5,[12] was the starting point. FAAH is a homodimer with active sites separated by ca. 40 Å. The present model includes one active site and all FAAH residues with any atom within 15 Å of it. Clipped residues were capped with acetyl or N-methylamine groups. The MAP inhibitor was replaced by a 2-pyridyl oxazolyl derivative of oleamide using the BOMB program.[45] The system was then subjected to conjugate-gradient energy minimization in order to relax the contacts between protein residues

(37) Jorgensen, W. L.; Maxwell, D. S.; Tirado-Rives, J. *J. Am. Chem. Soc.* **1996**, *118*, 11225−11236.
(38) Repasky, M. P.; Chandrasekhar, J.; Jorgensen, W. L. *J. Comput. Chem.* **2002**, *23*, 1601−1622.
(39) Tubert-Brohman, I.; Guimaraes, C. R. W.; Repasky, M. P.; Jorgensen, W. L. *J. Comput. Chem.* **2004**, *25*, 138−150.
(40) Tubert-Brohman, I.; Guimaraes, C. R. W.; Jorgensen, W. L. *J. Chem. Theory Comput.* **2005**, *1*, 817−823.
(41) Dewar, M. J. S.; Zoebisch, E. G.; Healy, E. F.; Stewart, J. J. P. *J. Am. Chem. Soc.* **1985**, *107*, 3902−3909.
(42) Stewart, J. J. P. *J. Comput. Chem.* **1989**, *10*, 221−264.
(43) Thompson, J. D.; Cramer, C. J.; Truhlar, D. G. *J. Comput. Chem.* **2003**, *24*, 1291−1304.
(44) Udier-Blagovic, M.; De Tirado, P. M.; Pearlman, S. A.; Jorgensen, W. L. *J. Comput. Chem.* **2004**, *25*, 1322−1332.
(45) Jorgensen, W. L. *BOMB*, version 2.5; Yale University: New Haven, CT.

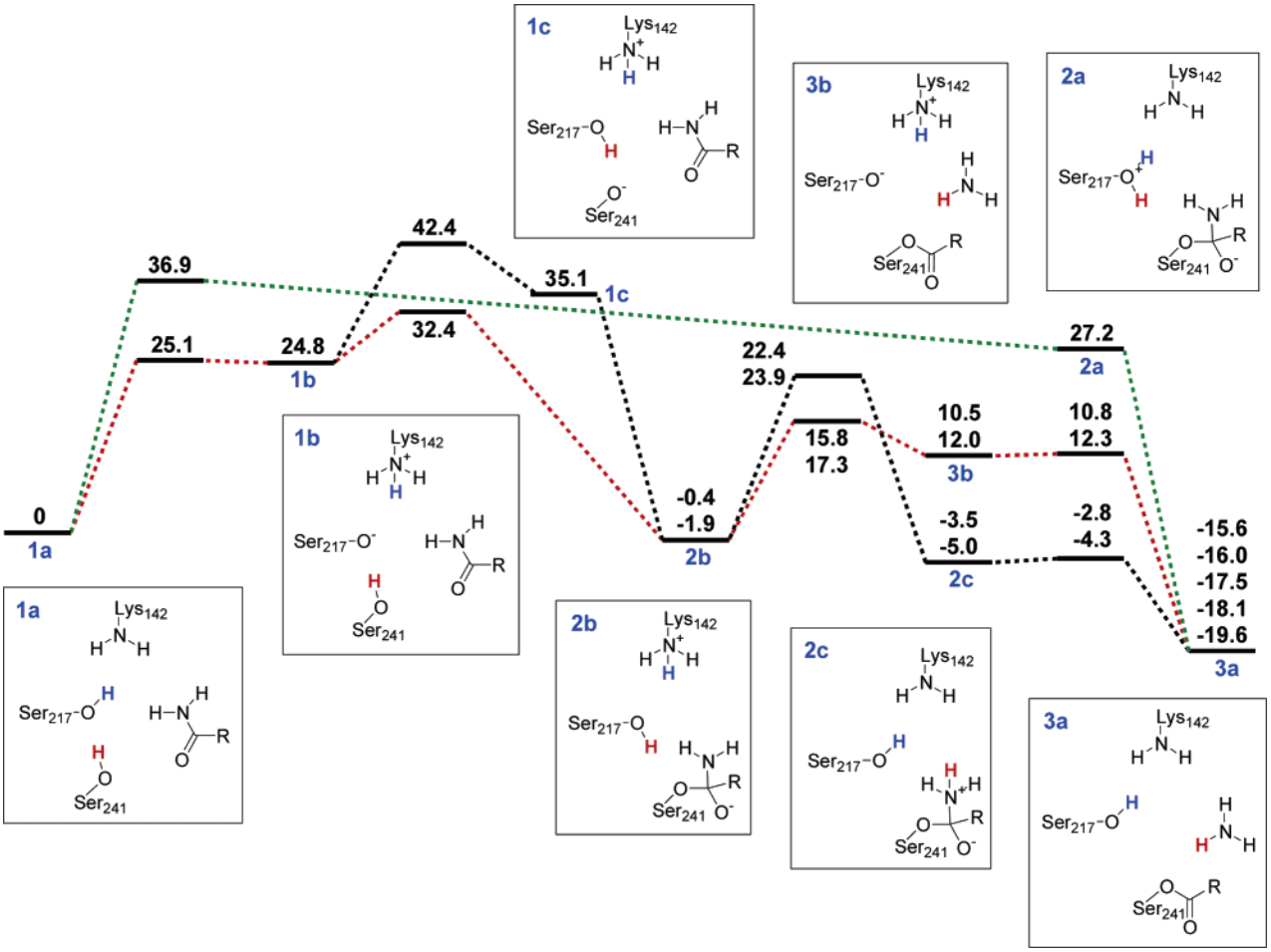


***Figure 8.*** Computed free-energy diagram for several mechanisms for formation of the acyl intermediate **3a** from the Michaelis complex **1a**. Mechanism **A** (**1a** → **1b** → **2b** → **3b** → **3a**) is highlighted in red, and mechanism **B** (**1a** → **2a** → **3a**) is highlighted in green. Free energy values are given in kcal/mol relative to **1a**.

and the substrate. For the present work, the oxazolyl inhibitor was converted to oleamide or methyl oleate by manual modification of the internal coordinate representation (Z-matrix). During the MC simulations, only the bond angles and dihedral angles of side chains of residues with any atom within 10 Å of the center of the system were varied. All degrees of freedom in the QM region were varied, except those adjacent to the link atom as discussed above and those involved in the reaction coordinates as discussed below.

The reduced FAAH model consists of 2680 atoms and 197 residues, out of the 537 in a single FAAH chain. The total charge of the system was set to zero by adjusting the protonation states of the residues farthest from the center of the system. The entire system was solvated with a 22-Å radius cap containing 617 TIP4P[46] water molecules; a half-harmonic potential with a force constant of 1.5 kcal mol$^{-1}$ Å$^{-2}$ was applied to water molecules at distances greater than 22 Å from the center of the system to prevent possible evaporation. The MM part of the protein was represented with the OPLS-AA force field,[37] using residue-based cutoffs of 10 Å for all nonbonded interactions.

As a side issue, the effect of the truncation and neutralization of FAAH on the electric potential ($E_j = \Sigma q_i e^2/r_{ij}$) near the active site was investigated. The electric potential for several atoms in the active site region was computed for one configuration of the reduced model and one of the full 537-residue FAAH chain with conventional charge assignments. The results are shown in Figure 4. The overall trend is similar for both models, but shifted by about 24 kcal mol$^{-1}$ e$^{-1}$ in the positive direction for the full-chain model, as expected due to its overall charge of +2. However, a constant shift in the electric potential, which would happen in the ideal case if the active site were placed inside a charged sphere, would not affect the results; only changes in the gradient of the electric potential (i.e., the electric field) would. There were some differences at the local level, such as for the O and H of Ser217, but they were found to be very sensitive to the specific configuration analyzed and are attributed mostly to close-range interactions with the substrate.

**PMF Calculations.** Potential of mean force (PMF) calculations were used to build free-energy profiles for several reaction pathways for formation of the acyl intermediate **3a** from the Michaelis complex **1a**, shown in Figure 5. The mechanism has been assumed to start with Lys142 in the deprotonated state, based on the pH activity profile of the enzyme.[13] In the PMF calculations, a reaction coordinate is driven by using free-energy perturbations[47] during Monte Carlo simulations. A series of "windows", each consisting of a small geometric perturbation, such as stretching a bond, are then combined to produce a one-dimensional (1D) free-energy profile or PMF. It is also possible to combine a PMF run along one reaction coordinate with a series of PMFs run along a second reaction coordinate to produce a two-dimensional (2D) PMF. A variety of 1D and 2D PMF calculations were used for this work, as indicated in Figure 5. Each 1D PMF calculation involving the formation or breaking of a bond between heavy atoms was split into ca. 30 windows with an increment of 0.04 Å in the reaction coordinate; the resolution of the PMF is half of the window

(46) Jorgensen, W. L.; Chandrasekhar, J.; Madura, J. D.; Impey, R. W.; Klein, M. L. *J. Chem. Phys.* **1983**, *79*, 926−935.

(47) (a) Zwanzig, R. W. *J. Chem. Phys.* **1954**, *22*, 1420−1426. (b) Jorgensen, W. L.; Ravimohan, C. *J. Chem. Phys.* **1985**, *83*, 3050−3056. (c) Kollman, P. A. *Chem. Rev.* **1993**, *93*, 2395−2417.

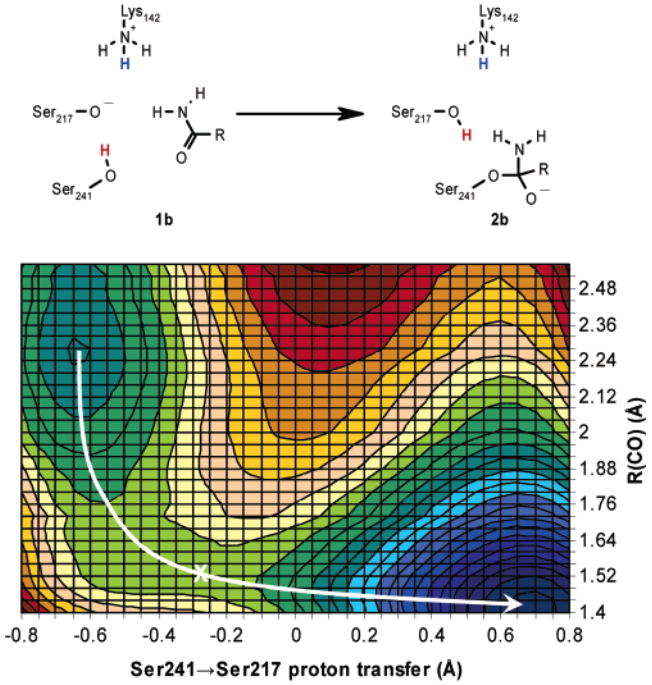


***Figure 9.*** 2D PMF for the transformation of **1b** to **2b**, the rate-determining step for mechanism **A** in the hydrolysis of oleamide by FAAH. The reaction coordinate for proton transfer is $R_{OH} - R_{O'H}$, with $R_{OH} + R_{O'H} = 2.60$ Å, where O′ is the Ser217 oxygen. The X marks the transition structure; contour lines are spaced every 2 kcal/mol.

size due to the use of double-wide sampling.[47b] For proton transfers, it was found that the free-energy changes for individual windows converge very well and can be fit almost perfectly by a cubic polynomial, as shown in Figure 6a. Analytical integration yields a quartic polynomial for the overall proton-transfer PMF. Using just 7 windows out of the usual 30 for the proton transfer and integrating yields essentially the same PMF as that from running the full 30 windows, as shown in Figure 6b. In this case, the largest deviation between the approximate and the detailed calculation was 0.5 kcal/mol; this value is used as an estimate of the uncertainty in the calculated free-energy changes that involved the polynomial approximation. The 2D PMFs that were done always involved a proton transfer as one of the reaction coordinates. This allowed the use of the quartic polynomial approximation in at least one direction; only 35 ($5 \times 7$) windows for the proton PMF were run, spaced evenly throughout the 2D surface. This reduces the number of windows required for a 2D PMF from about 900 to about 65, with little loss of accuracy. However, to obtain more precise estimates for the activation barriers associated with effects of the Lys142Ala mutation on the amide/ester selectivity ratio, some of the proton-transfer PMFs were refined using every window.

**Reaction Coordinates.** For the reaction steps involving the formation or breaking of a C−O or C−N bond, the reaction coordinate used for the PMF was simply $R_{CO}$ or $R_{CN}$. For proton transfers, a common approximation for simultaneous bond making and breaking was used to reduce the dimensionality of the problem.[18,20] As an example, the reaction coordinates for step 1a → 2a are shown in Figure 7a. For the proton transfer between Ser241 and Ser217, the reaction coordinate is $R_{OH} - R_{O'H}$, and $R_{OH} + R_{O'H}$ is kept constant at 2.6 Å. The fixed distance of 2.6 Å was determined from gas-phase studies of proton transfers and inspection of multiple configurations of the structure of the protein from the MC simulations. However, introducing a constraint in the PMF calculation can result in overestimation of the reaction barrier. To assess this, the gas-phase potential energy surface for the proton transfer between protonated methanol and methanol was computed using PDDG/PM3. As shown in Figure 7b, in this case, the actual value of $R_{OH} + R_{O'H}$ at the transition state is near 2.4 Å; and it is apparent that

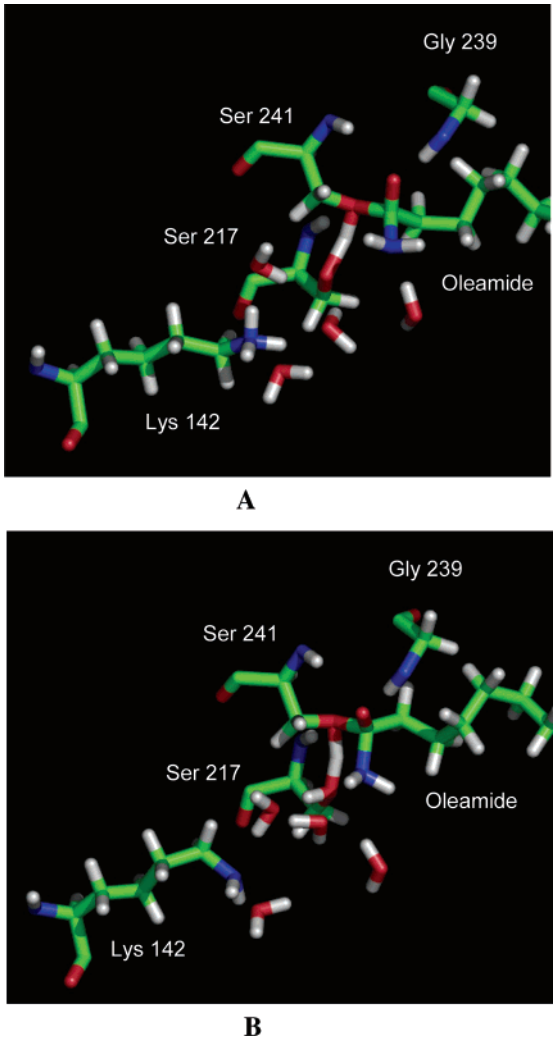


***Figure 10.*** Snapshots of the active site, taken at the end of MC simulations near the rate-determining transition states for mechanisms **A** and **B**. Ile240 is omitted for clarity.

with $R_{OH} + R_{O'H}$ fixed at 2.6 Å, the barrier is overestimated by about 1 kcal/mol. Gas-phase models for other relevant proton transfers were examined and found to display similar behavior. The overestimation is expected to remain constant when comparing different substrates or different mutations of the protein and, therefore, should not impact the present calculations of the ester/amide selectivity ratio.

**Monte Carlo Simulation Protocol.** All simulations were run at 25 °C using Metropolis Monte Carlo statistical mechanics. Each simulation for a FEP window consisted of $5 \times 10^6$ configurations of solvent relaxation, where the water molecules were moved randomly while keeping the protein and substrate fixed, followed by $10 \times 10^6$ configurations of full equilibration where all degrees of freedom were varied, and $25 \times 10^6$ or $50 \times 10^6$ configurations of averaging, where all degrees of freedom were sampled and the free-energy changes were obtained. The perturbations involving proton transfer were found to converge faster, so they used the shorter averaging periods. During the simulations, 10% of the attempted MC moves involved the solute, and 1% involved the QM region. Each move of the QM region requires one self-consistent field QM calculation if the move is rejected and three if the move is accepted (reference and two perturbed structures). Therefore, each FEP window required ca. $(0.5-1) \times 10^6$ QM calculations; the total for this work exceeded $500 \times 10^6$. This highlights the importance of having very fast QM energy and charge evaluation; this was made possible through the use of the PDDG/PM3 semiempirical method and a relatively small QM region.

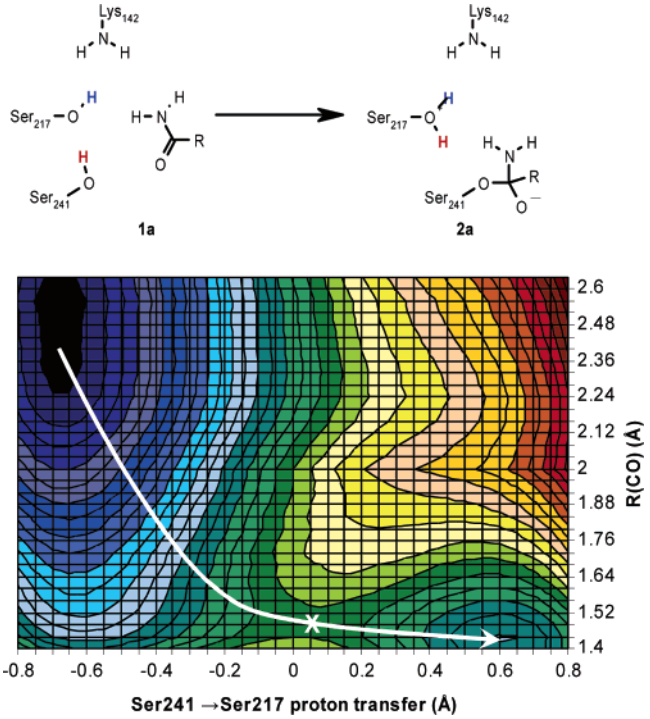


***Figure 11.*** 2D PMF for the transformation of **1a** to **2a**, the rate-determining step for mechanism **B** in the hydrolysis of oleamide by FAAH. Reaction coordinate for proton transfer is $R_{OH} - R_{O'H}$, with $R_{OH} + R_{O'H} = 2.60$ Å, where O′ is the Ser217 oxygen. The X marks the transition structure; contour lines are spaced every 2 kcal/mol.

## Results and Discussion

**Hydrolysis of Oleamide by Wild-Type FAAH.** The computed free-energy changes and barriers for each step of the oleamide hydrolysis mechanisms depicted in Figure 5 are listed in Table 1. These can be used to build the free-energy diagram shown in Figure 8. For the free energy of intermediates **2b**, **2c**, **3a**, and **3b**, slightly different values are obtained depending on the path used, and the deviations become larger the farther a state is from the initial state **1a**. However, a single value is obtained for the rate-determining free-energy barriers, which are found close to the beginning of the mechanisms.

The pathway **1a** → **1b** → **2b** → **3b** → **3a** is referred to here as mechanism **A**. For oleamide, it consists of (1) deprotonation of Ser217 by Lys142, (2) formation of the tetrahedral intermediate concerted with proton transfer from Ser241 to Ser217, (3) proton transfer from Ser217 to the $NH_2$ leaving group concerted with $NH_3$ elimination, and (4) protonation of the Ser217 alkoxide anion by the ammonium side chain of Lys142 to return to their initial states. Mechanism **A** is similar to the one proposed by McKinney and Cravatt.[13] It is also the one modeled by Lodola et al. up to the tetrahedral intermediate **2b**.[18] The concertedness of the process is different in the McKinney−Cravatt mechanism; they proposed that attack of Ser241 on the substrate's carbonyl occurs "in a coupled manner with proton donation from Ser-217 to the nitrogen atom of the amide substrate" and "coincidental donation of a proton from Lys142 to Ser217". Thus, in their mechanism the **1b** → **2b** → **3b** → **3a** sequence is folded into one concerted process without the explicit intervention of intermediate **2b** or **3b**. Related to this, additional possibilities were considered here including the stepwise formation of **2b** via **1c** and double proton transfer from **2b** to yield the zwitterionic **2c**, which could directly eliminate to the products. The alternative mechanism **B** (**1a** → **2a** → **3a**) was also studied since it does not involve participation by Lys142 and is expected to be viable for the Lys142Ala mutant. In this case, the process begins with simultaneous proton transfer from Ser241 to Ser217 and addition to the substrate, followed by simultaneous elimination and protonation of the leaving group.

The favored mechanism turns out to be **A** (Figure 8). Step 2 to yield the tetrahedral intermediate **2b** is rate-determining, and the overall calculated activation barrier is 32.4 kcal/mol. This is similar to the barrier of 36.0 kcal/mol obtained by Lodola et al. using PM3 and the CHARMM force field.[18] The two studies concur that formation of the tetrahedral intermediate is rate-determining and that **2b** is a true intermediate in a significant free-energy well. The similarities between the present results and those of Lodola et al. for the formation of the tetrahedral intermediate provide some mutual validation of the differing methodologies, though the computed barriers are overestimated relative to the experimental value of 16.0 kcal/mol.[13] Such overestimates are common for barrier heights of addition and pericyclic reactions with semiempirical methods.[20,26−28,35,38] However, the difference in barrier heights obtained here for the addition and elimination steps, 16 kcal/mol, is sufficiently large that it is unlikely that the conclusion that the former is rate-determining is erroneous. It may be noted that Lodola et al. then corrected their PM3-based energy surface leading to **2b** with results from B3LYP/6-31+G(d) single-point calculations, which reduced the activation energy to 18 kcal/mol.[18] Furthermore, corrections for quantum effects may be expected to lower the barriers for the present proton-transfer steps by up to a few kcal/mol.[20,48]

The 2D free-energy surface for the transformation of **1b** to **2b** is shown in Figure 9. It illustrates that the mechanism is concerted but asynchronous, with the C−O bond almost completely formed at the TS ($R_{CO} = 1.52$ Å), while the proton is still close to Ser241 ($R_{OH} - R_{O'H} = -0.25$ Å). Lodola et al. also found a concerted mechanism for this step, although their results were not completely explicit regarding the synchronicity due to a different choice of reaction coordinate.[18] A snapshot taken at the end of the Monte Carlo simulation near the **1b** to **2b** transition state is in Figure 10a. The figure shows the tetrahedral intermediate almost fully formed, while the proton is being transferred from Ser241 to Ser217. Other notable features include strong hydrogen bonds with the backbone HN of Ser242, Gly239, and Ile240 (the latter omitted from the figure for clarity), which form the oxyanion hole of the enzyme. There are also four water molecules near the reaction site which are involved in hydrogen bonds with Lys142, Ser217, and the nitrogen of oleamide. The presence of these water molecules is consistent with McKinney and Cravatt's speculation that water-bridged proton transfer may be involved in the reaction mechanism for the Ser217Ala mutant[13] and is necessary for the subsequent hydrolysis of the acyl intermediate.

Turning to mechanism **B**, the barrier is computed here to be 4.5 kcal/mol higher than for that for mechanism **A** (Figure 8). Because Lys142 does not participate in mechanism **B**, it is a feasible alternative when Lys142 is mutated to a nonbasic amino acid such as alanine. Indeed, the increase in the computed barrier height is comparable to the 6.8 kcal/mol increase found

(48) Pu, J.; Gao, J.; Truhlar, D. J. *Chem. Rev.* **2006**, *106*, 3140−3169.

***Table 2.*** Free Energies of Reaction and Activation (kcal/mol) for Steps in the Hydrolysis of Methyl Oleate by FAAH and for the Hydrolysis of Oleamide and Methyl Oleate by the Lys142Ala Mutant

| | WT/OME | | K142A/oleamide | | K142A/OME | |
|---|---|---|---|---|---|---|
| step | $\Delta G^{\ddagger}$ | $\Delta G$ | $\Delta G^{\ddagger}$ | $\Delta G$ | $\Delta G^{\ddagger}$ | $\Delta G$ |
| **1a** → **1b** | 25.7 ± 0.1 | 24.9 ± 0.1 | | | | |
| **1a** → **2a** | 33.9 ± 0.5 | 26.2 ± 0.5 | 40.1 ± 0.1 | 31.7 ± 0.5 | 35.2 ± 0.1 | 27.8 ± 0.5 |
| **1b** → **2b** | 4.9 ± 0.1 | −24.2 ± 0.5 | | | | |

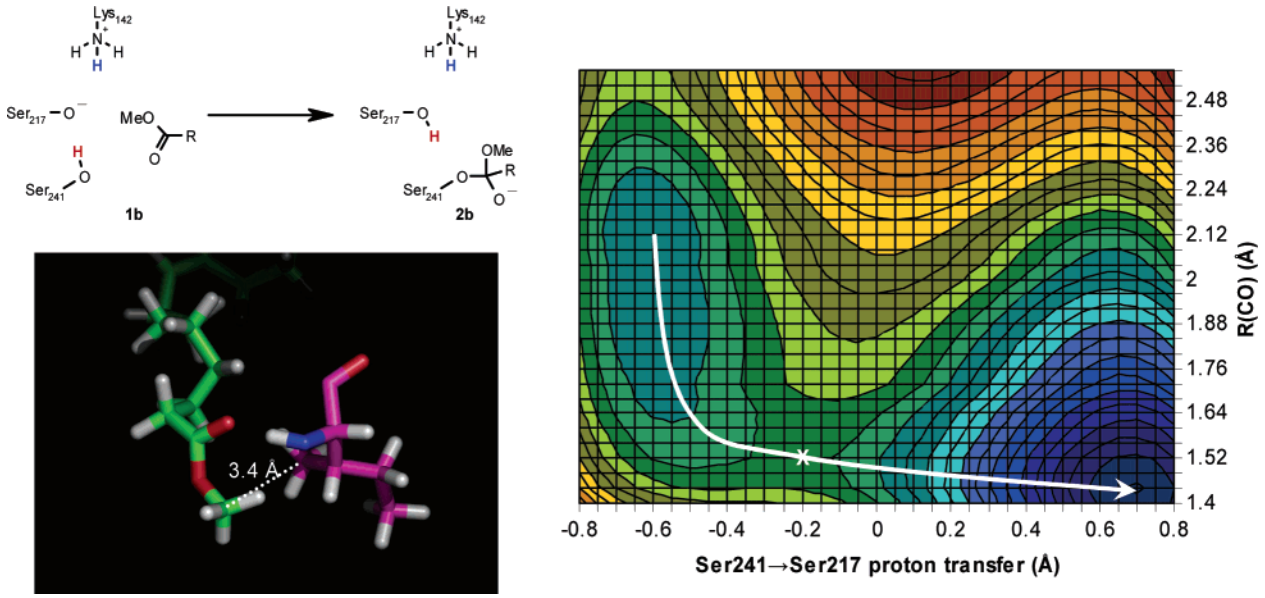


***Figure 12.*** 2D PMF for conversion of **1b** to **2b**, the rate-determining step for mechanism **A** in the hydrolysis of methyl oleate by FAAH. Reaction coordinate for proton transfer is $R_{OH} - R_{O'H}$, with $R_{OH} + R_{O'H} = 2.60$ Å, where O′ is the Ser217 oxygen. X marks the transition structure; contour lines are spaced every 2 kcal/mol. The snapshot on the left shows the interaction between methyl oleate and Ile240 near energy minimum **1b**.

experimentally upon mutation of Lys142 to Ala.[13] A snapshot from an MC simulation near the transition state is shown in Figure 10b, and the 2D free-energy surface for the rate-determining step for this mechanism is shown in Figure 11. This step, which involves C−O bond formation and proton transfer from Ser241 to Ser217, is also concerted and asynchronous. However, the proton transfer is more advanced at the transition state than for mechanism **A**; this is expected from Hammond's postulate, because the rate-determining step is now far more endergonic, leading to formation of a relatively unstable protonated alcohol in **2a**. The second step of mechanism **B**, the proton transfer from Ser217 to the oleamide nitrogen atom with concomitant elimination (**2a** → **3a**), is barrierless, suggesting that it is likely concerted with the first step. The molecular choreography in this case would then be a striking, cyclic dance.

**Methyl Oleate and the Lys142Ala Mutant.** To explore the origins of the differences in selectivity between oleamide and methyl oleate for FAAH and the Lys142Ala mutant, free-energy barriers were also computed for the rate-determining steps in the hydrolysis of methyl oleate with wild-type FAAH, as well as for the hydrolysis of oleamide and methyl oleate by the Lys142Ala mutant. For the reaction with wild-type FAAH, both mechanisms **A** and **B** were considered; for the mutant, only mechanism **B** was pursued since residue 142 is no longer capable of accepting a proton. The results for the individual steps are listed in Table 2. For mechanism **A**, an overall barrier of 29.8 kcal/mol (24.9 + 4.9) is obtained for the hydrolysis of methyl oleate by FAAH. This barrier is lower by 2.6 kcal/mol than the computed barrier for the hydrolysis of oleamide, while experimentally the barrier for the hydrolysis of oleamide is lower by 0.6 kcal/mol.[13] The free-energy change for the initial proton-transfer step **1a** → **1b**, 24.9 kcal/mol, is essentially identical to that for the same step of oleamide hydrolysis (24.8 kcal/mol). Inspection of the free-energy surface and structure for the addition step **1b** → **2b** of the ester hydrolysis (Figure 12) suggests that the underestimation of the computed barrier may be partially due to some steric compression of the starting state **1b**. As seen in the figure, the minimum for **1b**, when compared to that for oleamide hydrolysis (Figure 9), is flatter and shifted to a shorter $R_{CO}$ distance. This may result from crowding between the methyl group of methyl oleate and the side chain of Ile240, which is not relieved completely due to the rigidity

***Table 3.*** Relative $\Delta\Delta G^{\ddagger}$ for Mechanism **B** in Wild-Type FAAH and the Lys142Ala Mutant (kcal/mol)

| substrate | enzyme | calcd | expt[c] |
|---|---|---|---|
| oleamide | WT[a] | 0 | 0 |
| | WT[b] | 4.5 ± 0.2 | |
| | K142A | 7.7 ± 0.2 | 6.8 |
| methyl oleate | WT[a] | 0 | 0 |
| | WT[b] | 4.1 ± 0.2 | |
| | K142A | 5.4 ± 0.2 | 3.8 |

[a] Mechanism **A** (involves proton transfer to Lys142). [b] Mechanism **B** (does not involve proton transfer to Lys142). [c] Calculated from kinetic data from ref 13.

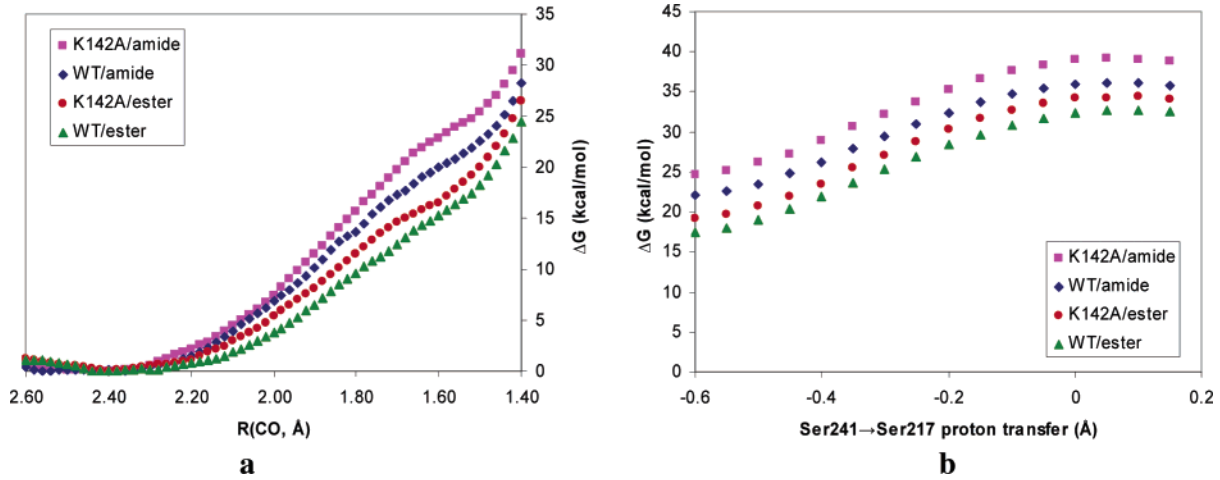


***Figure 13.*** Comparison of step **1a** → **2a** for the hydrolysis of oleamide and methyl oleate by wild-type FAAH and the Lys142Ala mutant, decomposed into two steps: (a) addition component, keeping the proton-transfer reaction coordinate fixed at −0.60 Å and (b) proton-transfer component, keeping $R_{CO}$ fixed at 1.52 Å.

of the protein backbone during the simulations. This also suggests the possibility that mutating Ile240 might have an effect on FAAH's selectivity.

For the Lys142Ala variant, hydrolysis is assumed to follow mechanism **B**, and the computed barriers for hydrolysis of oleamide and methyl oleate are 40.1 and 35.2 kcal/mol (Table 2). The changes in the barrier heights in comparison to wild-type FAAH are summarized in Table 3. The calculated increase for oleamide is 2.3 ± 0.3 kcal/mol larger than that for methyl oleate, which agrees well with the observed difference of 3.0 kcal/mol.[13] Thus, the mutation makes the ester hydrolysis relatively more facile, and the change in the amide/ester selectivity ratio is reproduced satisfactorily.

The most straightforward explanation for the change in amide/ester selectivity with FAAH and the Lys142Ala mutant focuses on the nucleophilicity of Ser241 for mechanisms **A** and **B**. For mechanism **A**, the proton transfer to Lys142 makes Ser241 a "hot" (stronger) nucleophile owing to its proximity to the Ser217 alkoxide and ease of proton transfer to it in progressing to **2b**. The hot Ser241 shows little selectivity between the amide and ester substrates. Then for the Lys142Ala mutant, mechanism **B** is followed, Ser241 is less activated by the neutral Ser217, and the usual amide/ester selectivity arises. Indeed, mechanism **A** does show an earlier TS for the proton transfer than mechanism **B** (Figures 9 and 11), and the proton-transfer step, **1a** → **1b**, accounts for most of the activation barrier (Figure 8).

Further support of the "hot" nucleophile proposal was obtained from additional FEP results for mechanism **B**. Specifically, the **1a** → **2a** conversion was decomposed using 1D PMFs into the carbonyl addition and then the Ser241 to Ser217 proton transfer, basically following a vertical line then a horizontal one instead of the white curve in Figure 11. The results are shown in Figure 13 for both substrates with FAAH and the Lys142Ala variant. It is apparent that the addition component is responsible for most of the divergence between the effects of the mutation on the hydrolysis of oleamide and methyl oleate; the free-energy profiles for the proton transfer are almost perfectly parallel and just shifted, indicating that neither the nature of the substrate nor the choice of Lys142 or Ala142 have a large influence on that component of the **1a** → **2a** conversion. The selectivity for mechanism **B** is controlled by the carbonyl addition step and reflects the normal higher reactivity of esters than amides, which is attributed to the greater resonance stabilization of amides. Overall, the computed and observed effects of the Lys142Ala mutation on the hydrolyses of oleamide and methyl oleate are also in reasonable accord (Table 3). However, the "hot" nucleophile effect is not strongly apparent in the computed results for the amide and ester using mechanism **B** in the presence of neutral Lys142. The activation barriers increase, but the change is only 0.4 kcal/mol greater for the amide than the ester. The steric environment is, of course, different in the active site than when residue 142 is neutral Lys or Ala. Though this computational result cannot be checked experimentally, it would be interesting to obtain rate data for additional Lys142 variants and to perform parallel computational studies. Data for one additional mutant of FAAH are available;[49] interestingly, the Lys142Glu variant is $10^3$−$10^4$-fold less active than FAAH but restores FAAH's lack of ester/amide selectivity and appears to be deacylation rate-limited.

## Conclusions

QM/MM/FEP simulations have been carried out for several possible pathways for the hydrolysis of oleamide by FAAH. The preferred mechanism (**A**) consists of proton transfer from Ser217 to Lys142, followed by the rate-determining step, which is the formation of the C−O bond between Ser241 and the substrate with concomitant proton transfer from Ser241 to Ser217. An alternative mechanism (**B**) that does not involve Lys142 but has a barrier that is higher by 4.5 kcal/mol was also found. In addition, mechanism **A** was also computed to be preferred for the hydrolysis of methyl oleate by FAAH. To assess the possibility that mechanism **B** occurs with the Lys142Ala mutant, which lacks the basic side chain on residue 142 that is required by mechanism **A**, simulations of the hydrolysis of oleamide and methyl oleate by the mutant were also performed. Indeed, the experimentally observed effects of

(49) Patricelli, M. P.; Cravatt, B. F. *Biochemistry* **1999**, *38*, 14125−14130.

the mutation on the hydrolysis rates are well-reproduced by following mechanism **A** for FAAH and mechanism **B** for the Lys142Ala variant. Mechanism **B** is a striking, multistep sequence with simultaneous proton transfer from Ser241 to Ser217, attack of Ser241 on the carbonyl carbon of the substrate, and elimination of the leaving group and its protonation by Ser217. The unusually high activity of FAAH toward oleamide vs methyl oleate is most readily attributed to enhancement of the nucleophilicity of Ser241 upon proton transfer from Ser217 to Lys142. The usual selectivity is restored in the Lys142Ala variant for which the acylation step is rate-dominating.

**Acknowledgment.** Gratitude is expressed to the National Institutes of Health (GM032136) and National Science Foundation (CHE-0446920) for financial support; to Prof. Dale L. Boger for discussions; and to Drs. Cristiano R. W. Guimarães, Julian Tirado-Rives, and Theresa M. Lyons for assistance.

JA065863S